

Phenomenological Rule from Correlations of Conduction/Valence Band Energies and Bandgap Energies in Semiconductor Photocatalysts: Calcium Bismuthates versus Strontium Bismuthates

D. S. Shtarev,^[a, b] V. K. Ryabchuk,^[c] A. V. Rudakova,^[d] A. V. Shtareva,^[a, b] M. S. Molokeyev,^[b, e, f] E. A. Kirichenko,^[g] and N. Serpone^{*,[h]}

A number of calcium bismuthates were synthesized (25 to 50 mol% in Ca) and characterized by XRD, SEM, EDX, XPS and DRS techniques; the latter provided an estimate of the bandgap energies (E_{bg} = 2.41 to 3.29 eV) via Tauc plots for indirect transitions, whereas XPS established the potentials (vs NHE) of their respective valence bands (and thus the conduction bands). Linear correlations existed between E_{VB}/E_{CB} and E_{bg} that when compared with those of strontium bismuthates (reported earlier) showed that differences in energies at $E_{bg} = 0$ eV are related to the difference in the absolute electronegativities of Ca and Sr, from which the following empirical phenomenological rule is postulated: replacing one alkaline earth metal in bismuthates by another causes the points of intersection of the linear correlations $E_{CB}(E_{bg})$ and $E_{VB}(E_{bg})$ to be displaced by an amount equal to twice the difference in absolute electronegativities of these metals.

In an earlier study,^[1] we demonstrated a novel trend in the empirical dependence of the conduction and valence band positions on the bandgap energy of semiconductors for alkali earth metal bismuthate photocatalysts.^[2] The dependences $E_{CB} = f(E_{bg})$ and $E_{VB} = f(E_{bg})$ for the bismuthates could be approximated by the linear functions $E_{CB} = A + B E_{bg}$ and $E_{VB} = a$

+ $b E_{bg}$, respectively, thereby illustrating that bismuthates of alkaline earth metals formed a new trend in the field of semiconductor photocatalysts. The novel trend was characterized by a distinct relationship between the energy position of the valence band and the conduction band on the one hand, and the bandgap energy on the other. In the aforementioned study,^[1] conclusions were reached on the basis of an analysis of the properties of three strontium bismuthates examined earlier in some detail by Shtarev and coworkers,^[2] and one calcium bismuthate investigated by Wang et al.^[3] It seemed of interest, therefore, to discover whether different alkaline earth metals (Sr versus Ca) in bismuthates might affect such observed linear dependence, and if so how.

Accordingly, a number of calcium bismuthates were synthesized (25 to 50 mol% in Ca) in this study and then characterized by XRD, SEM, EDX, XPS and DRS techniques, following which the linear correlations $E_{CB} = A + B E_{bg}$ and $E_{VB} = a + b E_{bg}$ were compared to the data on strontium bismuthates reported previously.^[1]

The X-Ray diffraction patterns of all as-synthesized samples of calcium bismuthates are displayed in Figure 1. All peaks were indexed by the corresponding unit cells from known structures of $Ca_5Bi_4O_{26r}$,^[4] $CaBi_2O_4r$,^[5] $Ca_4Bi_6O_{13r}$,^[6] and $Ca_2Bi_2O_5$.^[7] Consequently, these structures were taken as the starting model for the Rietveld refinement, which was performed using TOPAS

[a] Prof. D. S. Shtarev, Dr. A. V. Shtareva
Yu. A. Kosygin Institute of Tectonics and Geophysics
Far Eastern branch of the Russian Academy of Sciences
65 Kim Yu Chen Street
Khabarovsk 680063 (Russia)

[b] Prof. D. S. Shtarev, Dr. A. V. Shtareva, Dr. M. S. Molokeyev
Far Eastern State Transport University
47 Seryshev Street
Khabarovsk 680021 (Russia)

[c] Prof. V. K. Ryabchuk
Department of Photonics
Saint-Petersburg State University
Ul'yanovskaya 1
Saint-Petersburg 198904 (Russia)


[d] Dr. A. V. Rudakova
Laboratory Photoactive Nanocomposite Materials
Saint-Petersburg State University
Ul'yanovskaya 1
Saint-Petersburg 198904 (Russia)

[e] Dr. M. S. Molokeyev
Kirensky Institute of Physics
Akademgorodok 50, bld. 38
Krasnoyarsk 660036 (Russia)

[f] Dr. M. S. Molokeyev
Siberian Federal University
79 Svobodny pr.
Krasnoyarsk 660041 (Russia)

[g] Dr. E. A. Kirichenko
Institute of Materials Science
Khabarovsk Scientific Center
Far East Branch of the Russian Academy of Sciences
153 Tihookeanskaya Street
Khabarovsk 680000 (Russia)

[h] Prof. N. Serpone
PhotoGreen Laboratory
Dipartimento di Chimica
Università di Pavia
via Taramelli 12
Pavia 27100 (Italia)
E-mail: nick.serpone@unipv.it

 Supporting information for this article is available on the WWW under <https://doi.org/10.1002/cctc.201902236>

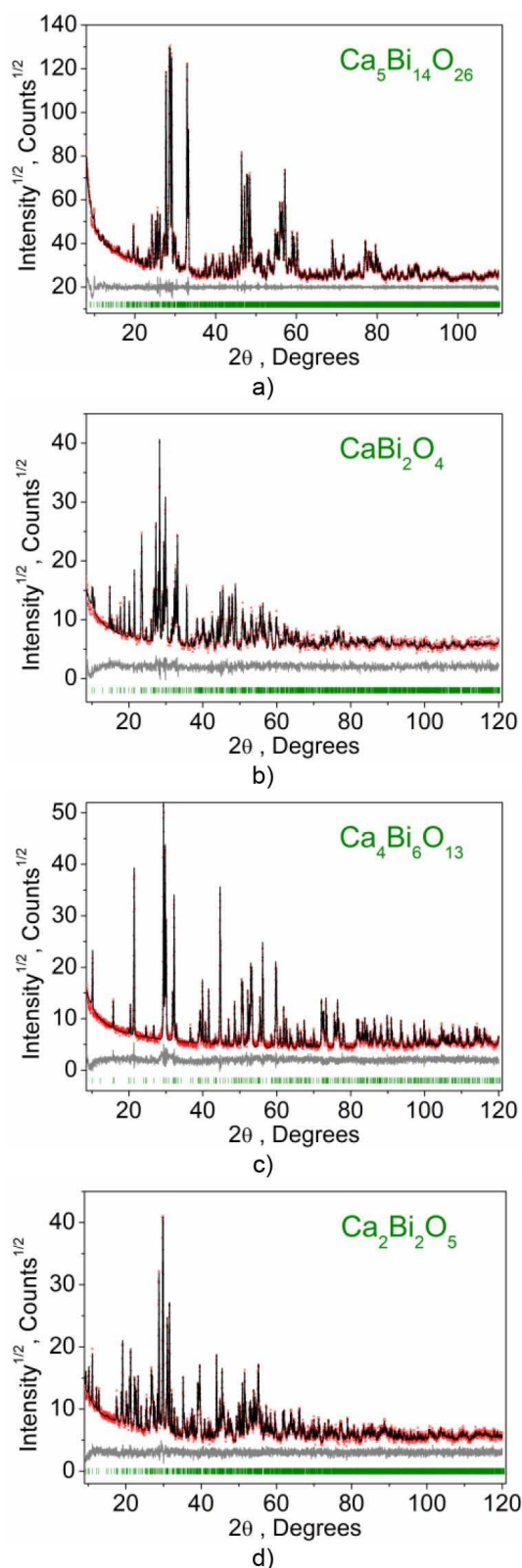


Figure 1. Difference Rietveld plots of the as-prepared calcium bismuthates: (a) Ca₅Bi₁₄O₂₆, (b) CaBi₂O₄, (c) Ca₄Bi₆O₁₃, and (d) Ca₂Bi₂O₅.

4.2.^[8] Refinements were stable and gave low *R*-factors (see Table S1 in Supporting Information). All samples were therefore proven to be rather pure.

The morphologies of the particles of the as-synthesized calcium bismuthates were examined by the SEM technique. Figures S2–S5 show typical particles of various calcium bismuthates obtained during the pyrolytic synthesis. All particles displayed a sponge-like form with a developed surface and a large number of pores, a consequence of the synthesis technique used. It is during the pyrolysis of the organic matrix that a large number of pores were formed. The uniform distribution of the individual elements over the particle volume was confirmed by the EDX method (Figures S6–S9), which was also used to ascertain the elemental composition. For this, the particles were deposited on a microscope stage with a dense layer (see Figure S10), from which the EDX spectrum was recorded. Results of the analysis are presented in Table S2. Clearly, the chosen synthesis method allowed for the calcium bismuthate samples to achieve a stoichiometric ratio between elements in the cationic sub-lattice.

The bandgap energies of all the calcium bismuthates were determined from DRS spectra given as absorbance versus wavelength as illustrated in Figure S11. Both Ca₂Bi₂O₅ and Ca₅Bi₁₄O₂₆ exhibit significant absorption in unusual spectral regions, while the calcium bismuthates CaBi₂O₄ and Ca₄Bi₆O₁₃ display no such features. The bandgap energies of the respective calcium bismuthates were determined by Tauc plots considering the Kubelka–Munk transformation for indirect electronic transitions (Figure 2); relevant bandgaps are also reported in the inset.

The oxidation states of the elements Ca, Bi, and O in the bismuthates were ascertained from XPS spectra for Ca 2*p*, Bi 4*f* and O 1*s* reported in Figures S12–S14. The spectral curves for Ca 2*p* are rather complex and can be described by the sum of two bands displaced from each other (Figure S12). The band located in the region of lower binding energies exhibits a maximum at 347 eV, which corresponds to calcium with an oxidation state of +2 in the structure of a number of complex oxides.^[9] The second band with maximum shifted to 350–

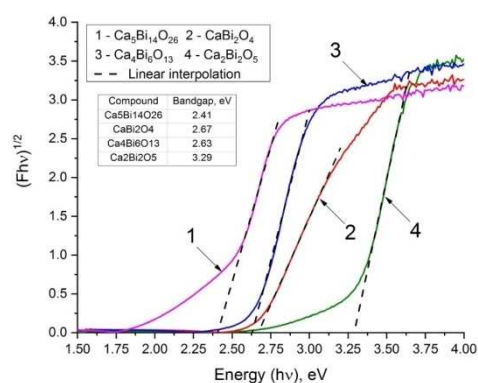


Figure 2. Tauc plots for all the as-synthesized calcium bismuthate samples for indirect transitions. The E_{bg} values (E at $F_{hv} = 0$) and the corresponding measurement errors for the bismuthates (Table 1) were obtained using a least squares approximation at the linear portion of the $F(E)$ curves.

351 eV also corresponds to calcium with an oxidation state of +2 albeit it is associated with a carbonate structure,^[9] as alkaline earth metals tend to absorb carbon dioxide from the air. A similar situation was observed on the surface of samples with chemically sorbed carbon dioxide in a number of strontium bismuthates.^[2]

The Bi 4*f* XPS spectra of the calcium bismuthates consist of two well resolved bands corresponding to Bi 4*f*_{7/2} and Bi 4*f*_{5/2} (Figure S13). In all calcium bismuthates, bismuth exhibits an oxidation state of +3. The binding energies of the Bi 4*f*_{7/2} and Bi 4*f*_{5/2} band maxima are in good accord with published data.^[10] In addition, the bismuth bands can be described by a single Gaussian, which infers that the adsorption of carbon dioxide on the surface of the samples occurs precisely because of the presence of calcium.

The O 1*s* spectra of the calcium bismuthates are rather complex and is described by the sum of two bands (Figure S14). The lower intensity band corresponds to the binding energy of 529.4–529.5 eV that is characteristic of oxygen with an oxidation state of –2 in complex oxides (e.g., in calcium chromate; see ref. [9]). The second band shifted toward higher energies to 531.9–532.1 eV, corresponds to oxygen with an oxidation state of –1. A large number of oxygen in an oxidation state of –1 seems likely characteristic of bismuthates of alkaline earth metals – similar results were shown previously for a number of strontium bismuthates,^[2] for which oxygen with an oxidation state of –1 was associated with the displacement of oxygen from normal lattice sites to interstitial positions.

The energies of the respective valence bands of the four bismuthates were determined from the low-energy band edge of the O 2*p* XPS spectra (Figure 3) in accordance with the method proposed by Chambers and coworkers,^[10] binding energies are given versus the NHE scale as were those reported earlier for the strontium bismuthates.^[1]

The bandgap energies E_{bg} and the energies of the valence bands, E_{VB} , measured for all the calcium bismuthates allow us to calculate the values of the conduction band energies E_{CB} (Table 1). The data are also illustrated graphically in Figure 4.

Clearly, the strontium bismuthates and the calcium bismuthates appear to display their own characteristic trends in the mutual arrangement in plots of E_{CB} and E_{VB} versus E_{bg} , which are well described by the linear relationships (Equations 1a and 1b):

$$E_{CB} = \mathbf{A} + \mathbf{B}E_{bg} \quad (1a)$$

$$E_{VB} = \mathbf{a} + \mathbf{b}E_{bg} \quad (1b)$$

where **A**, **B**, **a**, and **b** are constants.

The numeric values of the parameters of the linear correlations presented in Figure 4 are listed in Table 2. Several interesting and important features can be highlighted from an analysis. First, both calcium and strontium bismuthates are characterized by the observation that the difference between slopes (**B-b**) equals 1. For instance, in the case of the strontium bismuthates (**B-b**) = –1.73 – (–0.73) = –1.00, while for calcium bismuthates (**B-b**) = –0.84 – (0.16) = –1.00.

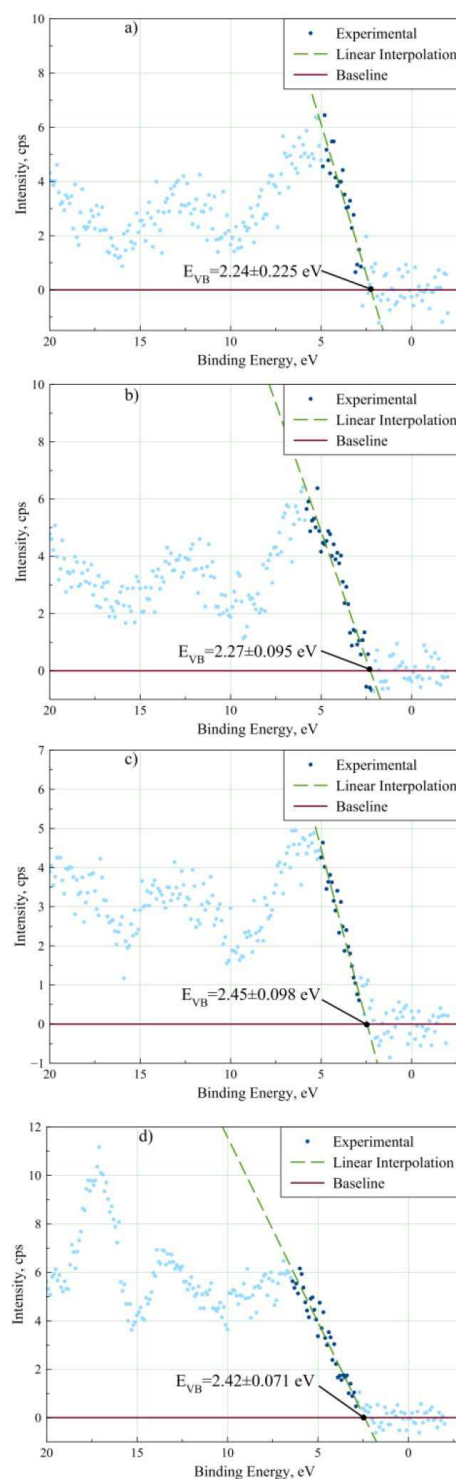


Figure 3. XPS spectra of the O 2*p* bands for the calcium bismuthates: (a) $\text{Ca}_5\text{Bi}_{14}\text{O}_{26}$, (b) CaBi_2O_4 , (c) $\text{Ca}_4\text{Bi}_6\text{O}_{13}$, and (d) $\text{Ca}_2\text{Bi}_2\text{O}_5$.

Also, for both identified trends, the intersection of the lines $E_{CB}(E_{bg})$ and $E_{VB}(E_{bg})$ at the point corresponding to $E_{bg}=0$ is rather characteristic. Lines $E_{CB}(E_{bg})$ and $E_{VB}(E_{bg})$ for the strontium bismuthates intersect at an energy of 4.07 eV, whereas for the calcium bismuthates they intersect at an energy of 1.90 eV (Figure 4). Such a decrease in energy of 2.17 eV is no doubt

Table 1. Bandgap energies and energies of the valence and conduction bands versus NHE with zero at pH=7 for the as-synthesized calcium bismuthates.

Sample	E_{bg} [eV]	E_{VB} [eV]	E_{CB} [eV]
$Ca_5Bi_{14}O_{26}$	2.41 ± 0.12	2.24 ± 0.23	-0.17 ± 0.34
$CaBi_2O_4$	2.67 ± 0.02	2.27 ± 0.09	-0.40 ± 0.11
$Ca_4Bi_6O_{13}$	2.63 ± 0.09	2.45 ± 0.10	-0.18 ± 0.19
$Ca_2Bi_2O_5$	3.29 ± 0.08	2.42 ± 0.07	-0.87 ± 0.15

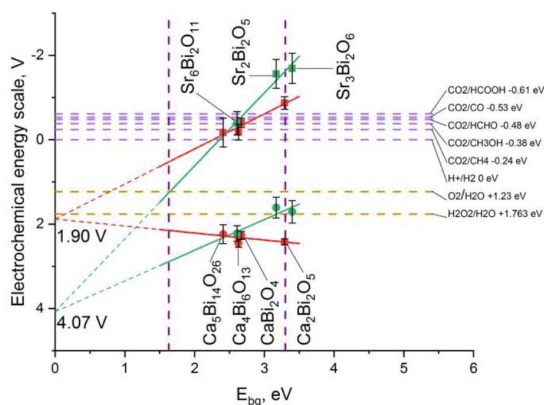


Figure 4. Positions of the conduction band energies (E_{CB}) and of the valence band energies (E_{VB}) as a function of the bandgap energy (E_{bg}) for the set of calcium and strontium bismuthates. The data reported as filled red squares and circles correspond to the calcium bismuthates, whereas the data illustrated as filled green squares and circles correspond to the strontium bismuthates reported earlier by Shtarev et al.^[11] The red and green solid lines correspond to the linear correlations $E_{CB}(E_{bg})$ and $E_{VB}(E_{bg})$ for calcium and strontium bismuthate, respectively. The red and green dashed lines show the extrapolation of the resulting correlations to the intersection points at $E_{bg} = 0$ eV. The blue (at 3.3 eV) and red (at 1.63 eV) dashed vertical lines denote the limits of visible light. The horizontal dashed lines correspond to reduction (violet) and oxidation (yellow) half-reactions.

Table 2. Approximation parameters (A, B, a, b) for the two sets of bismuthates.

Parameters	$A \pm \Delta A$ $a \pm \Delta a$	$B \pm \Delta B$ $b \pm \Delta b$	Data from
Strontium Bismuthates			
E_{CB} [eV]	4.07 ± 1.06	-1.73 ± 0.34	[1]
E_{VB} [eV]	4.07 ± 1.06	-0.73 ± 0.34	
Calcium Bismuthates			
E_{CB} [eV]	1.90 ± 0.44	-0.84 ± 0.16	Current study
E_{VB} [eV]	1.90 ± 0.44	0.16 ± 0.16	

related to replacement of strontium by calcium in the elemental composition of the bismuthates.

According to the theory of Butler and Ginley,^[11] the semiconductor energies E_{CB} and E_{VB} depend on the absolute electronegativity (in the Mulliken sense) of the elements, in the present case Sr and Ca. Such absolute electronegativity is defined by the arithmetic mean between the electron affinity E_{ea} of an element and its corresponding ionization energy E_{Ii} :

$$\chi = \frac{|E_{Ii} + E_{ea}|}{2} \quad (2)$$

Thus, if we take the ionization energies of the elements summarized by Kramida and coworkers,^[12] and the electron affinities for Sr and Ca by Andersen et al.^[13] and Petrunin et al.,^[14] respectively, then application of Equation 2 yields: $\chi_{Sr} = 5.3565$ eV and $\chi_{Ca} = 4.2400$ eV. Consequently, calcium is 1.1165 eV less electronegative than strontium.

It is clear from Figure 4 that replacing Sr by Ca in the bismuthates shifted the point of intersection of the lines $E_{CB}(E_{bg})$ and $E_{VB}(E_{bg})$ in the linear correlations that led to a decrease in energy by 2.17 eV. Remarkably, half this decrease is 1.085 eV, nearly identical to the calculated difference of 1.1165 eV from the absolute electronegativities of calcium and strontium. It is tempting, therefore, to propose the following empirical phenomenological rule: replacing one alkaline earth metal in bismuthates by another causes the points of intersection of the linear correlations $E_{CB}(E_{bg})$ and $E_{VB}(E_{bg})$ to be displaced by an amount equal to twice the difference in absolute electronegativities of these metals. It would be of interest to examine additional ternary oxides to establish whether this rule also applies to other such systems.

Experimental Section

The calcium bismuthates were synthesized using chemically pure bismuth(III) nitrate pentahydrate, $Bi(NO_3)_3 \cdot 5H_2O$, calcium nitrate tetrahydrate, $Ca(NO_3)_2 \cdot 4H_2O$, and sorbitol $C_6H_{14}O_6$ (purity > 99%). These precursors were ground to a transparent viscous solution owing to the water of crystallization of crystalline hydrates. The quantities of calcium and bismuth nitrates were calculated based on their molar ratios in the resulting calcium bismuthate. The mass of sorbitol used was 1.5 times greater than the calculated mass of the resulting calcium bismuthate. The resulting viscous solution was allowed to rest for a day at ambient temperature during which time nitration of sorbitol took place that was accompanied by the transformation of the transparent viscous liquid into a yellow solid foamy mass. This mass was subsequently ground for homogenization and subjected to pyrolysis at 200 °C to decompose the organic component. Annealing of the residual pyrolytic carbon was carried out by stepwise isothermal aging at 450, 500, 550, 600 °C for 1 h at each stage. The final heat treatments of the synthesis of the targeted phases were carried out at 650–700 °C for 24 hrs.

The as-prepared calcium bismuthates were located in the range from about 25 to 50 mol% in calcium (see phase diagram in Figure S1^[15]): namely, $Ca_5Bi_{14}O_{26}$ (26.3 mol%), $CaBi_2O_4$ (33.3 mol%), $Ca_4Bi_6O_{13}$ (40 mol%), and $Ca_2Bi_2O_5$ (50 mol%).

The powder diffraction data used for the Rietveld analysis were collected at room temperature using a Rigaku MiniFlex II powder diffractometer (Cu-K α radiation): step size of 2 θ angle was 0.05 degrees, and the counting time was 1 s per step.

The morphologies of the bismuthate particles were determined by Scanning Electron Microscopy (SEM) on a TESCAN Microscope (Czech Republic; acceleration voltage, 30 kV). The elemental compositions and their distribution within the samples were established by Energy Dispersive X-ray Spectroscopy (EDX; X-Max^N, Oxford Instruments, UK).

The oxidation states of the elemental components of the as-prepared bismuthate samples together with the flatband energies of the corresponding valence bands (VB) were determined by X-ray Photoelectron Spectroscopy (XPS) using a Thermo Fisher Scientific Escalab 250Xi spectrometer (Al K α radiation, 1486.6 eV; spectral resolution, 0.5 eV); the reference carbon line C_{1s} (C–C bond) was taken at a binding energy of 284.8 eV.

Diffuse reflectance spectra, as R(λ), were recorded in the 300–800 nm spectral range under ambient conditions on a Cary 5000 UV/vis/NIR spectrophotometer equipped with a DRA 2500 external diffuse reflectance accessory; optical-grade BaSO₄ powder was the reference standard.

Acknowledgements

The research was supported from a grant from the Russian Science Foundation (project No. 19-73-10013). We are very grateful to the staff of the Khabarovsk Innovation and Analytical Center of the Yu. A. Kosygin Institute of Tectonics and Geophysics FEB RAS, and of the Research Center on Nanophotonics and the Center for Physical Methods of Surface Investigation (to Dr. Alexandra Koroleva) of the Research Park at Saint-Petersburg State University for their valuable assistance in carrying out the research and in providing the needed equipment. VKR and AVR acknowledge financial support from a grant by the Saint-Petersburg State University (Pure ID 39054581). One of us (NS) thanks Prof. A. Albin and the staff of the PhotoGreen Laboratory of the University of Pavia for their continued hospitality.

Conflict of Interest

The authors declare no conflict of interest.

Keywords: calcium bismuthates · strontium bismuthates · bandgap energies · semiconductor photocatalysts · linear correlation of E_{CB}/E_{VB} with E_{bg}

- [1] D. S. Shtarev, A. V. Shtareva, V. K. Ryabchuk, A. V. Rudakova, N. Serpone, *ChemCatChem* **2019**, *11*, 3534–3541; <https://doi.org/10.1002/cctc.201900439>.
- [2] D. S. Shtarev, A. V. Shtareva, V. K. Ryabchuk, A. V. Rudakova, P. D. Murzin, M. S. Molokheev, A. V. Koroleva, A. I. Blokh, N. Serpone, *Catal. Today* **2020**, *340*, 70–85; <https://www.DOI:10.1016/j.cattod.2018.09.035>.
- [3] Y. J. Wang, Y. M. He, T. T. Li, J. Cai, M. F. Luo, L. H. Zhao, *Catal. Commun.* **2011**, *18*, 161–164.
- [4] B. Burton, C. Rawn, R. Roth, N. J. H. Wang, *Res. Nat. Inst. Stand. Technol.* **1993**, *98*, 469.
- [5] I. N. Sora, W. Wong-Ng, Q. Huang, R. S. Roth, C. J. Rawn, B. P. Burton, A. Santoro, *J. Solid State Chem.* **1994**, *109*, 251–258.
- [6] J. B. Parise, C. C. Torardi, M. H. Whangbo, C. J. Rawn, R. S. Roth, B. P. Burton, *Chem. Mater.* **1990**, *2*, 454–458.
- [7] J. B. Parise, C. C. Torardi, C. J. Rawn, R. S. Roth, B. P. Burton, A. Santoro, *J. Solid State Chem.* **1993**, *102*, 132–139.
- [8] Bruker AXS TOPAS V4: General profile and structure analysis software for powder diffraction data – User's Manual, Bruker AXS, Karlsruhe, Germany, **2008**.
- [9] NIST X-ray Photoelectron Spectroscopy Database (Standard Reference Database 20, Version 4.1): <https://srdata.nist.gov/xps/>.
- [10] S. A. Chambers, T. Droubay, T. C. Kaspar, M. Gutowski, M. van Schilf-gaarde, *Surf. Sci.* **2004**, *554*, 81–89.
- [11] M. A. Butler, D. S. Ginley, *J. Electrochem. Soc.* **1978**, *125*, 228–232.
- [12] A. Kramida, Yu. Ralchenko, J. Reader, NIST ASD Team, *NIST Atomic Spectra Database* (ver. 5.7.1), **2019**; Available online at <https://physics.nist.gov/asd> (accessed November 20, 2019); National Institute of Standards and Technology, Gaithersburg, MD; <https://doi.org/10.18434/T4W30F>.
- [13] H. H. Andersen, V. V. Petrunin, P. Kristensen, T. Andersen, *Phys. Rev. A* **1997**, *55*, 3247–3249; <https://www.doi:10.1103/PhysRevA.55.3247>.
- [14] V. V. Petrunin, H. H. Andersen, P. Balling, T. Andersen, *Phys. Rev. Lett.* **1996**, *76*, 744–747; <https://www.doi:10.1103/PhysRevLett.76.744>.
- [15] B. Hallstedt, L. J. Gauckler, *Computer Coupling of Phase Diagrams and Thermochemistry*, **2003**, *27*, 177–191.

Manuscript received: November 30, 2019
Revised manuscript received: December 30, 2019
Accepted manuscript online: January 2, 2020
Version of record online: January 22, 2020